AGU PUBLICATIONS

Geophysical Research Letters

RESEARCH LETTER
10.1002/2013GL058861

Key Points:
- Lightning-induced electron precipitation occurs first in conjugate hemisphere
- Lightning spectral density necessary to understand all ionospheric effects
- Early VLF event/long-recovery occurrence not function of peak current and location

Correspondence to:
M. Gołkowski,
mark.golkowski@ucdenver.edu

Citation:
Gołkowski, M., N. C. Gross, R. C. Moore, B. R. T. Cotts, and M. Mitchell (2014), Observation of local and conjugate ionospheric perturbations from individual oceanic lightning flashes, *Geophys. Res. Lett.*, *41*, 273–279, doi:10.1002/2013GL058861.

Received 28 NOV 2013
Accepted 7 JAN 2014
Accepted article online 9 JAN 2014
Published online 30 JAN 2014

Observation of local and conjugate ionospheric perturbations from individual oceanic lightning flashes

M. Gołkowski[1], N. C. Gross[1], R. C. Moore[2], B. R. T. Cotts[3], and M. Mitchell[2]

[1]Department of Electrical Engineering, University of Colorado Denver, Denver, Colorado, USA, [2]Department of Electrical and Computer Engineering, University of Florida, Gainesville, Florida, USA, [3]Electrical Engineering and Computer Science Practice, Exponent, Inc., Bowie, Maryland, USA

Abstract Very low frequency (VLF) remote sensing observations of multifaceted local and conjugate ionospheric perturbations from geographically identified and well-characterized oceanic lightning discharges are presented for the first time. Lightning-induced electron precipitation (LEP) events are shown to produce disturbances first in the conjugate hemisphere and subsequently in the hemisphere of the causative lightning discharge in agreement with theoretical predictions. A rough threshold peak current of ~100 kA is identified for lightning discharges to generate LEP events for the geomagnetic conditions present during observations. The occurrence of early VLF events and the subsequent duration of their recovery do not seem to fit any simple metric of lightning discharge peak current or proximity to great circle path. Knowledge of the full spectral density of the lightning electromagnetic pulse, not just its peak current, and the subionospheric mode structure are likely necessary to determine if a specific lightning discharge will generate an early VLF perturbation.

1. Introduction

The effects of lightning discharges on the lower ionosphere have been actively studied for the last 30 years [*Inan et al.*, 2010, and references therein]. Perturbations induced by lightning discharges can be classified by three primary source mechanisms: electromagnetic pulse (EMP) effects, quasi-electrostatic (QE) effects, and lightning-induced whistler wave effects. The direct interaction of the EMP generated by the lightning return stroke with the ionosphere causes local ionospheric electron temperature and density changes, which are currently understood to be behind the optical emissions known as elves. The QE field established by the charge removal in the cloud to ground discharge are behind the phenomena of sprites and halos. The third type of mechanism is the most indirect and stems from the injection of the lightning electromagnetic energy into the magnetosphere and subsequent resonant interactions of these whistler mode waves with trapped radiation belt electrons. The wave-particle interaction causes some of the radiation belt electrons to impinge on the ionosphere in what is known as a lightning-induced electron precipitation (LEP) event. We also note that lightning is additionally associated with the production of gamma rays. However, the effects of such terrestrial gamma ray flashes (TGFs) on the ionosphere have not yet been comprehensively investigated.

The two primary tools of observation of lightning-induced ionospheric effects have been optical and very low frequency (VLF) remote sensing as these are the only techniques for sensing the *D* region nighttime ionosphere. VLF remote sensing involves observing perturbations in amplitude and phase of subionospherically propagating radio signals and thus provides observation capability over large geographic areas. Two types of VLF signatures are LEP events and early VLF events. While LEP events are caused by the LEP phenomena as their name implies, early events have, in various cases, been shown to be caused either by EMP [*Cheng and Cummer*, 2005] or QE [*Moore et al.*, 2003] mechanisms. Furthermore, some early VLF events can have extremely long recoveries lasting up to tens of minutes [*Cotts and Inan*, 2007]. Despite many years of work, outstanding questions remain regarding the timing of LEP perturbations, the physics of long-recovery events, and effects in the conjugate hemisphere. Significant improvements in global lightning detection technology in the last decade [*Dowden et al.*, 2002; *Said et al.*, 2010] have enabled identification and characterization of the causative lightning discharge including its precise time of occurrence even in the case of oceanic lightning. We present unique observations of the first local and conjugate ionospheric

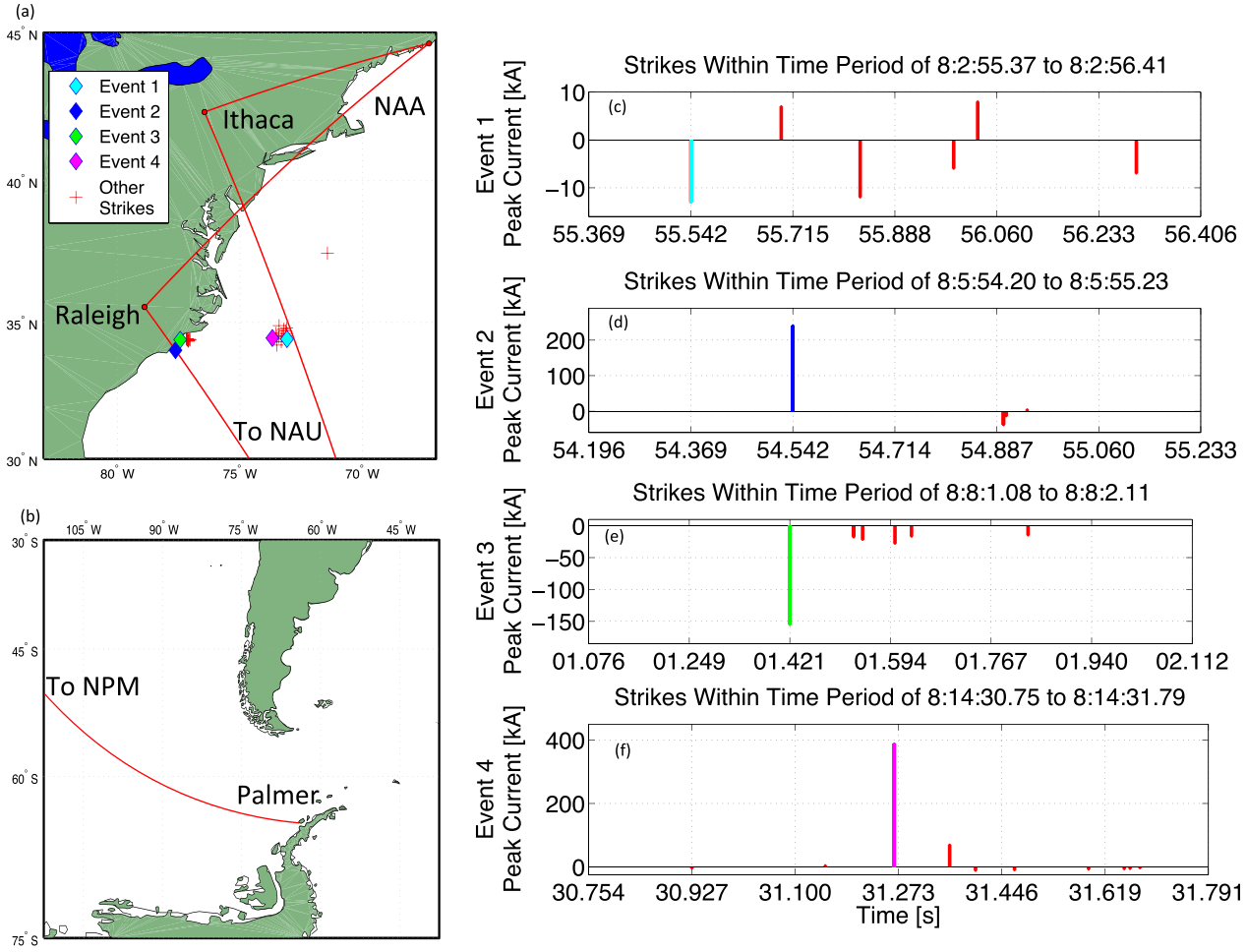

Figure 1. (a and b) Maps showing location of causative CG discharges for Events 1–4 (see Figure 2 and text) along with all other strikes in Figures 1c–1f. (c–f) Timing of each causative CG (shown in its respective color according to Figure 1a) along with all other CG discharges during select time interval shown in red.

disturbances of individual oceanic lightning discharges using VLF remote sensing. Results show that effects of a single cloud-ground (CG) discharge can be multifaceted and not easily predicted solely from CG peak current estimates.

2. Observations

VLF receivers systems located in the eastern United States and at Palmer Station, Antarctica are used to observe the amplitude and phase of narrowband VLF transmitter signals originating in Maine, USA (NAA: 24 kHz); Puerto Rico (NAU: 40.75 kHz), and Hawaii (NPM: 21.4 kHz). Maps of transmitter and receiver locations and connecting great circle paths can be seen in Figures 1 and 4. The VLF receivers consist of magnetic loop antennas, a preamplifier, a line receiver, and a digitizing computer. Receivers are sensitive to magnetic fields in the frequency range of ~300 Hz to ~47 kHz. Signals are sampled at a rate of 100 kHz with 16 bit resolution, while accurate timing is provided by a GPS-trained oscillator with 10^{-12} frequency precision. The mixed to baseband amplitude and phase of VLF transmitter signals are processed in real time and recorded at 50 Hz. Lightning location and peak current estimates are from the Vaisala Global Lightning Dataset (GLD360) [*Said et al.*, 2010].

Figure 2 shows the four Events of interest observed on 24 July 2012 8:00–8:15 UT. We use the capitalized word "Event" to describe multifaceted perturbations (LEP and early VLF events) resulting from a single CG discharge. Figures 2a–2c show the amplitude of the VLF transmitter signals received in the Northern Hemisphere (NAU– Ithaca [42.35°N and 76.44°W] and NAA–Raleigh [35.55°N and 78.89°W] and

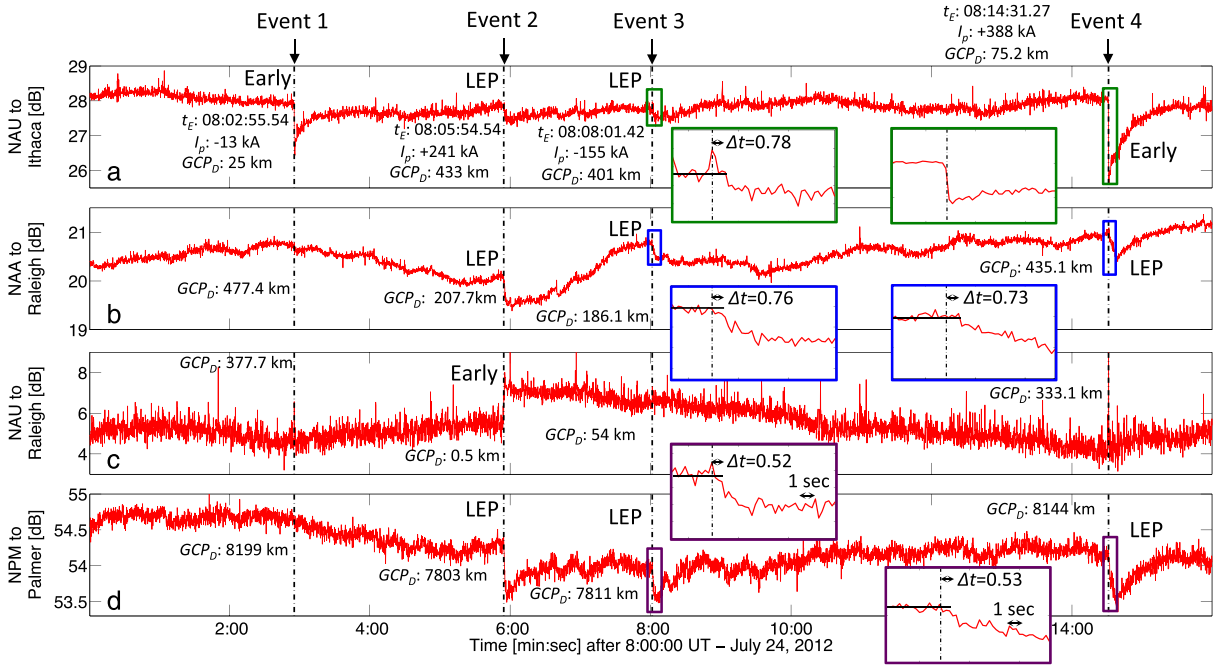

Figure 2. VLF amplitude data from the (a–c) Northern Hemisphere and the (d) southern conjugate hemisphere. Data for each Event are shown, where t_E, GCP_D, and I_p are the time of causative CG, distance between causative CG and transmitter-receiver path, and the peak current, respectively. The six insets show expanded time axis plots for Events 3 and 4 corresponding to boxes in larger panels. The dashed vertical line indicates the time of the causative CG for each Event obtained from the GLD360 network. Data are median filtered; higher time resolution data with visible causative spherics for Events 1 and 4 are shown in Figure 3.

NAU–Raleigh). Figure 2d shows the amplitude of NPM observed at Palmer Station [64.77°S and 64.05°W] along a great circle path in the southern conjugate hemisphere. The vertical dashed lines show the time of the causative CG discharges observed over the Atlantic Ocean; basic parameters of causative CGs are also shown in the figure including distance to each transmitter-receiver great circle path. Event 1 is an early VLF event observed on the NAU–Ithaca path. Events 2 and 3 are LEP events observed first in the Southern Hemisphere, followed by LEP events observed on both paths in the Northern Hemisphere. Additionally, Event 2 also has an early VLF event on the NAU–Raleigh path. Event 4 is seen to generate an early VLF event on the NAU–Ithaca path and then LEP events in the conjugate region (NPM–Palmer) and subsequently in the northern hemisphere (NAU–Raleigh). The geographic location of each causative CG as well as other concurrent CGs are shown in Figure 1.

For Event 3 and 4, the time difference between the conjugate (first) and local (second) LEP events can be seen to be ~0.24 s and ~0.2 s, respectively, as seen in the expanded time axis insets in Figure 2. The timing of the LEP event onset was determined by identifying the beginning of sustained departure from the ambient amplitude which is identified with a black line in the insets. Timing results for all observed disturbances, including onset delay (Δt), onset duration (t_d), and recovery duration(t_r), as well as perturbation magnitude (ΔA) are summarized in Table 1.

Events 2–4 have causative CG peak currents at least an order of magnitude higher than the CG associated with Event 1, and this is likely the reason that these events generate LEP events whereas Event 1 does not. Moreover, as can be seen in Figure 1, Events 2–4 have CG discharges with the highest peak current of all other CG discharges occurring in the vicinity during the time of observations. These observations thus indicate the existence of a peak current threshold for observable LEP event generation, which for our observation period is seen to be in the vicinity of 100 kA. Since the occurrence of LEP events is known to be strongly dependent on radiation belt fluxes [*Peter et al.*, 2006], the quantitative value of this threshold is expected to vary with geomagnetic conditions as well as geographic location.

Events 1 and 4 see the generation of early VLF events on the NAU–Ithaca path and Event 2 generates an early VLF event with a long recovery on the NAU–Raleigh path. We have not identified any definitive lightning characteristics that would explain why the CG discharges associated with these events cause early VLF

Table 1. VLF Signal Perturbation Parameters for Events 1-4 Including Onset Delay (Δt), Onset Duration (t_d), and Recovery Duration(t_r), Perturbation Magnitude (ΔA)[a]

Event	Path	Δt (s)	t_d (s)	ΔA (dB)	t_r (s)
1	NAU to Ithaca	0.04	0.5	1.7	17
	NAU to Ithaca	0.58	0.8	0.6	65
2	NAA to Raleigh	0.58	0.9	0.6	65
	NAU to Raleigh	0.02	0.04	1.9	260
	NPM to Palmer	0.42	1	0.9	30
	NAU to Ithaca	0.78	1.1	0.4	13
3	NAA to Raleigh	0.76	1.1	0.3	12
	NPM to Palmer	0.52	1	0.6	20
	NAU to Ithaca	0.004	0.004	2.1	45
4	NAA to Raleigh	0.73	2.2	0.6	32
	NPM to Palmer	0.53	2.1	0.8	31

[a]Onset duration is time difference between sustained departure from ambient value to maximum amplitude deviation. Recovery duration is time from maximum amplitude deviation to return within 10% of ambient amplitude. For the case of a highly disturbed path with multiple perturbations, the recovery duration is estimated via an exponential extrapolation of the recovery rate.

events and other CG discharges do not. Although Event 4 is caused by a very strong +CG of 388 kA, the CG of Event 1 is a modest −13 kA. The distance of the CG to the great circle path for these events are 25 km and 75 km, and as can be seen in Figure 1, there were numerous CGs closer to the NAU−Ithaca path that did not generate any observed perturbations. The early VLF event on the NAU−Raleigh path (Event 2) was generated by a CG within 0.5 km distance and in this case it was the closest and largest CG to the great circle path. Thus, while close proximity and large peak current appear to be correlated to early event occurrence, it is not possible to say anything definitive nor quantitative. In this regard, our observations seem to support the recent conclusions of *NaitAmor et al.* [2013] who found that the modal structure of the subionospheric VLF signal can be more important than the causative lightning stroke properties in determining the characteristics of VLF perturbations. At the same time, it is also possible that other not easily observable properties of the causative lightning flash may also play a role, such as the power spectral density of the lightning current discussed below.

We further analyzed the two early VLF observations from Events 1 and 4 using the scattered field decomposition technique put forth by *Dowden et al.* [1996]. As shown in Figure 3c, this technique utilizes the observed perturbations to the amplitude and phase of the VLF signal to isolate the field that is scattered from the lightning-induced ionospheric disturbance. Figures 3a and 3b show the changes in observed amplitude, phase, and derived scattered amplitude. Although the observed slow change of amplitude of Event 1 appears to suggest a so-called early/slow VLF event, the scattered field amplitude (3c) shows that the field is scattered abruptly (<20 ms) as in an early/fast VLF event. Thus, all of our observed early VLF events are of the early/fast type. Despite the difficulty in obtaining the required accurate VLF phase data, our observations strongly suggest the necessity of performing the scattered field decomposition for accurate identification and categorization of early VLF events.

3. Numerical Simulation of Electron Precipitation

The LEP events are simulated using models of the electron precipitation as well as ionospheric deposition and density change processes. Following the methodology of *Bortnik et al.* [2006], we use the Whistler-Induced Particle Precipitation (WIPP) code to calculate the pitch angle scattering by nonducted whistler mode waves. Using the calculated pitch angle scattering over the first 2 s of precipitation we then calculate the altitude profile of the ionospheric deposition using the atmospheric backscatter code (ABS) developed by *Cotts et al.* [2011a]. While the WIPP code uses a simple dipole model of the geomagnetic field, the ABS code uses an International Geomagnetic Reference Field model with longitudinal dependence and conjugate asymmetry of the bounce loss cone. The ABS code also takes into account the backscatter of particles that results when particles just within the loss cone impinge on the upper layers of the ionosphere.

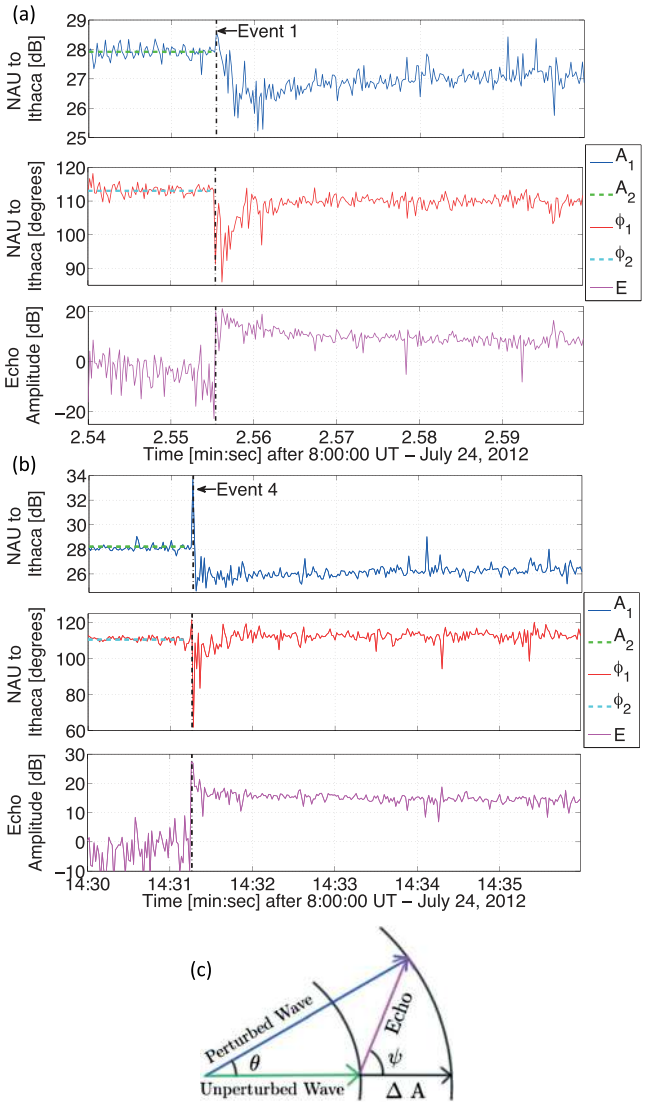

Figure 3. Scattered field decomposition for early VLF perturbations from (a) Events 1 and (b) 4. (c) Phasor diagram of the scattered field decomposition.

The WIPP code provides the pitch angle change of electrons with time resolution of 20 ms but does not track the particle trajectories after the brief wave-particle interaction. The ABS code accurately tracks the particle dynamics after the interaction, including multiple bounces, but has time resolution limited by the initial integration of the first 2 s of precipitation from the WIPP code.

Results of both codes are shown in Figure 4: flux scattered into the loss cone (<1000 km mirror altitude) from the WIPP code and ionospheric deposition from the ABS code. The results show general agreement with the observations. Specifically, the ABS code predicts a greater ionospheric perturbation in the Southern Hemisphere. This is in qualitative agreement with the larger amplitude changes for LEP events observed on the NPM-Palmer path as shown in Figure 2, even though, in general, the amplitude of VLF perturbations is also affected by the mode structure of the VLF signal. At the same time, it is somewhat surprising that in the southern hemisphere, the raw precipitation results from the WIPP code, which use the simple dipole model of the geomagnetic field, yield geographic locations that better match the geography of the observed perturbations. Specifically, the WIPP code predicts a perturbation on the NPM-Palmer great circle path as observed, while the ABS code predicts a perturbation on the NLK-Palmer path that was not observed.

The finer discrepancy between the models and the observations could be a result of the specific spectral content of the lightning discharge current waveforms being different than the model inputs. *Cotts et al.*

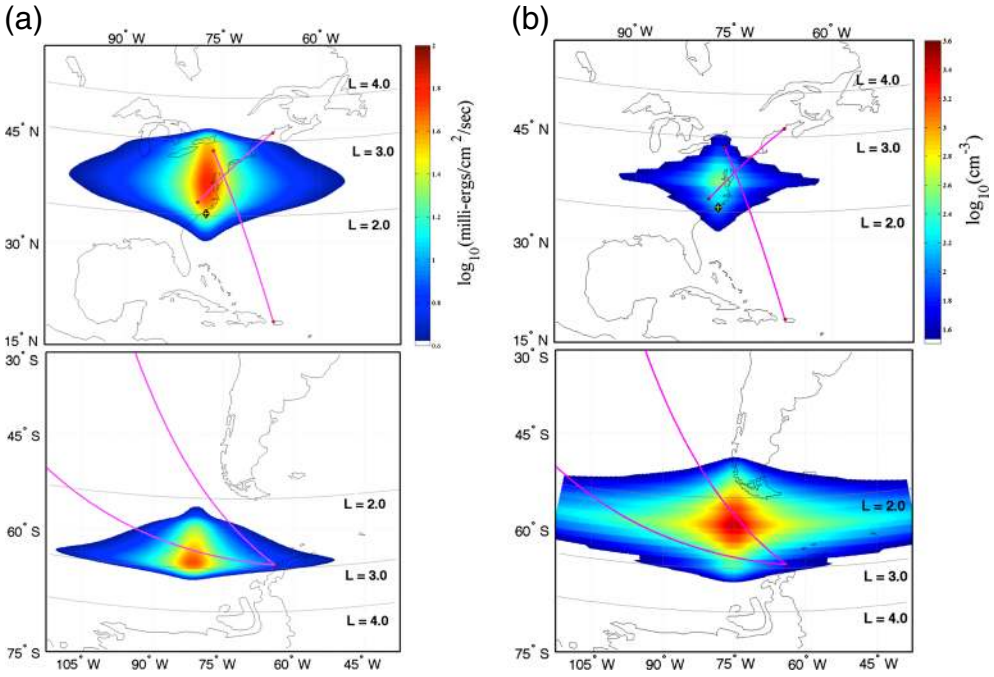

Figure 4. Numerical simulation results for Event 4 over first 2 s. (a) Electron precipitated flux from the WIPP code. (b) Density enhancement at an altitude of 80 km from the ABS code.

[2011b] show that the power spectral density of causative lightning discharges can have a significant effect on the location of the ionospheric perturbations from LEP events. Unfortunately, the GLD360 network provides only an estimate of the peak current of CG discharges and no information on the spectral content of the current waveform. For our simulations we used the standard two parameter double exponential analytical model [*Cotts et al.*, 2011b] of the lightning current waveform with a and b values of 10^4 and 5×10^4 chosen to give the closest possible match to the observations.

The 0.16−0.24 s delay between LEP perturbations in the Southern and Northern Hemisphere can be used to estimate the bounce period of precipitating electrons and hence their energy. This calculation depends on the L-shell of the precipitating particles. Using our maximum and minimum observed durations for a single magnetospheric traverse (half bounce period, τ_{hb}) and the observed L-shell span of precipitation: [0.24 s, $L = 2.5$] < [τ_{hb}, L] < [0.16 s, L= 3.0], we obtain the following bounds on electron energy: 90 keV< E <900 keV. This energy range is consistent with energies required for D region perturbations and corresponds to the range of precipitated electron energies from the simulations. We are not able to verify the τ_{hb} values directly with the codes since the high-resolution WIPP code does not track the trajectories after the wave-induced scattering and the trajectory tracking in the ABS code is based on a 2 s fluence input from the WIPP code [*Cotts et al.*, 2011a].

4. Discussion

Our observations and analysis confirm that for LEP events, the ionospheric perturbation in the conjugate ionosphere precedes the perturbation in the hemisphere of the causative lightning discharge by fractions of a second. These ground observations confirm the conjugacy of LEP phenomena previously observed only on spacecraft [*Voss et al.*, 1998].

Out of three observed early VLF events only one exhibited a long recovery. In a recent report *Haldoupis et al.* [2013] claim that for lightning discharges located within a 250 km of a great circle path of a transmitter-receiver pair, "the probability of occurrence (of long-recovery early events) increases with stroke intensity and approaches unity for discharges with peak currents 300 kA". Our observations of a lack of a long recovery for a +388 kA CG within 75 km of the great circle path suggest that the certainty of this conclusion about long-recovery occurrence put forth by *Haldoupis et al.* [2013] should be reassessed.

5. Summary

We present the first ground observations of simultaneous conjugate and local LEP events from single known lightning discharges. Our observations provide the first experimental evidence that for LEP events the initial ionospheric disturbance does in fact occur in the hemisphere conjugate to the causative CG discharge. The importance of scattered field analysis using both amplitude and phase data is highlighted by our observations. The occurrence of early VLF events and the subsequent duration of their recovery do not seem to fit any simple metric of lightning discharge peak current or proximity to great circle path. Knowledge of the subionospheric signal mode structure and full spectral density of the lightning EMP not just its peak current are likely necessary to determine definitively if a specific CG will generate an early VLF perturbation and how long its recovery will last. The spectral density can also more accurately predict the location of expected LEP induced ionospheric perturbations. In this context, nighttime rocket triggered lightning experiments that provide a direct measurement of the return stroke current would be extremely useful for future VLF remote sensing studies.

Acknowledgments

The authors would like to thank Ryan Said and Vaisala for access to the GLD360 data set. The authors additionally thank receiver hosts Czeslaw Golkowski of Super Pulse in Ithaca, NY and Eura Carpenter near Raleigh, NC. This work is supported by DARPA grant HR0011-10-1-0061 to the University of Florida and by subcontract UF-EIES-1005017-UCD to University of Colorado Denver. Further support is provided by NSF grants AGS-0940248 and PLR-1246275 to the University of Florida.

The Editor thanks two anonymous reviewers their assistance in evaluating this paper.

References

Bortnik, J., U. S. Inan, and T. F. Bell (2006), Temporal signatures of radiation belt electron precipitation induced by lightning-generated MR whistler waves: 1. Methodology, *J. Geophys. Res.*, *111*, A02204, doi:10.1029/2005JA011182.

Cheng, Z., and S. A. Cummer (2005), Broadband VLF measurements of lightning-induced ionospheric perturbations, *Geophys. Res. Lett.*, *32*, L08804, doi:10.1029/2004GL022187.

Cotts, B. R. T., U. S. Inan, and N. G. Lehtinen (2011a), Longitudinal dependence of lightning-induced electron precipitation, *J. Geophys. Res.*, *116*, A10206, doi:10.1029/2011JA016581.

Cotts, B. R. T., M. Gołkowski, and R. C. Moore (2011b), Ionospheric effects of whistler waves from rocket-triggered lightning, *Geophys. Res. Lett.*, *38*, L24805, doi:10.1029/2011GL049869.

Cotts, B. R. T., and U. S. Inan (2007), VLF observation of long ionospheric recovery events, *Geophys. Res. Lett.*, *34*, L14809, doi:10.1029/2007GL030094.

Dowden, R. L., J. B. Brundell, and W. A. Lyons (1996), Are VLF rapid onset, rapid decay perturbations produced by scattering off sprite plasma?, *J. Geophys. Res.*, *101*(D14), 19,175–19,183, doi:10.1029/96JD01346.

Dowden, R. L., J. B. Brundell, and C. J. Rodger (2002), VLF lightning location by time of group arrival (TOGA) at multiple sites, *J. Atmos. Sol. Terr. Phys.*, *64*, 817–830, doi:10.1016/S1364-6826(02)00085-8.

Haldoupis, C., M. Cohen, E. Arnone, B. Cotts, and S. Dietrich (2013), The VLF fingerprint of elves: Step-like and long-recovery early VLF perturbations caused by powerful ±CG lightning EM pulses, *J. Geophys. Res. Space Phys.*, *118*, 5392–5402, doi:10.1002/jgra.50489.

Inan, U. S., S. A. Cummer, and R. A. Marshall (2010), A survey of ELF and VLF research on lightning-ionosphere interactions and causative discharges, *J. Geophys. Res.*, *115*, A00E36, doi:10.1029/2009JA014775.

Moore, R. C., C. P. Barrington-Leigh, U. S. Inan, and T. F. Bell (2003), Early/fast VLF events produced by electron density changes associated with sprite halos, *J. Geophys. Res.*, *108*(A10), 1363, doi:10.1029/2002JA009816.

NaitAmor, S., M. B. Cohen, B. R. T. Cotts, H. Ghalila, M. A. AlAbdoadaim, and K. Graf (2013), Characteristics of long recovery early VLF events observed by the North African AWESOME Network, *J. Geophys. Res. Space Phys.*, *118*, 5215–5222, doi:10.1002/jgra.50448.

Peter, W. B., M. W. Chevalier, and U. S. Inan (2006), Perturbations of midlatitude subionospheric VLF signals associated with lower ionospheric disturbances during major geomagnetic storms, *J. Geophys. Res.*, *111*, A03301, doi:10.1029/2005JA011346.

Said, R. K., U. S. Inan, and K. L. Cummins (2010), Long-range lightning geo-location using a VLF radio atmospheric waveform bank, *J. Geophys. Res.*, *115*, D23108, doi:10.1029/2010JD013863.

Voss, H. D., M. Walt, W. L. Imhof, J. Mobilia, and U. S. Inan (1998), Satellite observations of lightning-induced electron precipitation, *J. Geophys. Res.*, *103*(A6), 11,725–11,744, doi:10.1029/97JA02878.